

Plasmonic Trace Sensing below the Photon Shot Noise Limit

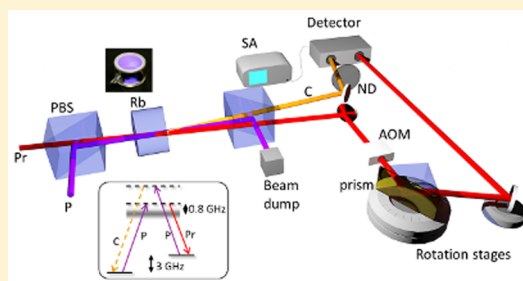
Raphael C. Pooser* and Benjamin Lawrie

Quantum Information Science Group, Computational Science and Engineering Division, Oak Ridge National Laboratory, Oak Ridge, Tennessee 37830, United States

S Supporting Information

ABSTRACT: Plasmonic sensors are important detectors of biochemical trace compounds, but those that utilize optical readout are approaching their absolute limits of detection as defined by the Heisenberg uncertainty principle in both differential intensity and phase readout. However, the use of more general minimum uncertainty states in the form of squeezed light can push the noise floor in these sensors below the shot noise limit (SNL) in one analysis variable at the expense of another. Here, we demonstrate a quantum plasmonic sensor whose noise floor is reduced below the SNL in order to perform index of refraction measurements with sensitivities unobtainable with classical plasmonic sensors. The increased signal-to-noise ratio can result in faster detection of analyte concentrations that were previously lost in the noise. These benefits are the hallmarks of a sensor exploiting quantum readout fields in order to manipulate the limits of the Heisenberg uncertainty principle.

KEYWORDS: plasmonics, quantum sensors, quantum plasmonics, surface plasmon resonance sensors, quantum optics



Quantum sensors are devices whose sensitivity has been augmented by quantum mechanical properties. They may rely on a field transducer constructed from a quantum mechanical object, such as cold atoms,^{1,2} or on a readout field exploiting quantum statistics.³ The study of quantum sensors has become a diverse and important field of general interest due to its broad applicability to research including gravitational wave interferometry,^{4,5} bioimaging,⁶ plasmonic imaging,⁷ displacement sensors,^{8,9} and myriad other detection schemes.^{10,11} In the classical regime, surface plasmon resonance (SPR) sensors have also found widespread application for medical, defense, and basic research purposes. However, as these devices approach their ultimate classical noise limits due to the Heisenberg uncertainty principle¹² in terms of both intensity¹³ and phase readout,¹⁴ quantum sensors will be required for further improvements in sensitivity. Previous work demonstrated detection of an index of refraction change of 0.014 using a plasmonic nanoparticle sensing platform combined with single photon optical readout, requiring long integration times in the presence of thermal noise.¹⁵ However, typical SPR sensors utilize bright fields for increased sensitivity and reduced acquisition time.

The current state of the art in SPR sensing utilizes balanced detection to remove any classical noise present in the probe field via subtraction of a reference field that does not interact with the plasmon.^{13,14,16} It is also possible to remove technical noise that is present at dc in these sensors through a well-known technique that uses a modulation on the probe field, allowing measurements to be performed at the modulation frequency^{17,18} via a lock-in amplifier or spectrum analyzer, for instance. However, the Heisenberg uncertainty principle for the intensity and phase of light imposes a quantum shot noise limit

(SNL) associated with the noise of the coherent state that cannot be surpassed with classical states.³ Indeed, while correlated classical noise can be subtracted at a balanced detector, shot noise adds in quadrature.³ On the other hand, two light fields sharing quantum correlations can be used to demonstrate quantum noise reduction below the photon SNL.^{19,20} This quantum noise reduction below the SNL is frequently referred to as “squeezing”, and when the noise reduction is the result of quantum correlations between two modes, the collection of modes are referred to as “two-mode squeezed states”. Amid growing interest in utilizing quantum states of light in nanoplasmonic applications,²¹ several authors have recently shown that both surface plasmon polaritons and localized surface plasmons are capable of transducing these intensity squeezed states.^{7,22} Here we show that bright states of light with macroscopic intensities exhibiting two-mode squeezing can be used as the optical readout field in a plasmonic sensor in order to drastically increase the sensitivity within the same integration time window as the corresponding classical sensor. The increased signal-to-noise ratio (SNR) resulting from the sub-SNL noise floor results in faster detection of a given particle concentration or in the detection of smaller concentrations that were previously lost in the noise for the same integration time. This compact and robust approach to quantum sensing can be applied to any SPR sensing geometry to outperform the optimum classical measurement.

The most ubiquitous plasmonic sensor (the widely adopted Kretschmann configuration,²³ see Figure 1a) consists of

Received: September 9, 2015

Published: December 9, 2015

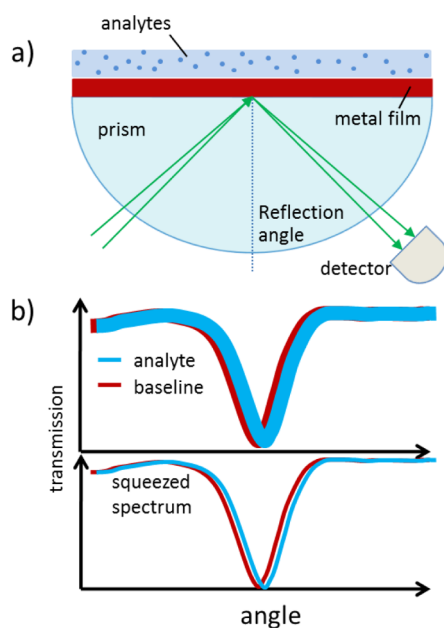


Figure 1. (a) SPR sensor consisting of a prism, metal coating on the back side, a readout light field, and a detector that reads angular shift. (b) Schematic showing intensity and noise of a reflective SPR sensor as a function of angle.

plasmon polaritons supported on metal films that evanescently couple to optical fields through intermediary prisms. These devices detect a change in the concentration of an agent of interest by registering a shift in the plasmonic response to the local index of refraction at the film's surface. When incident light reflects from the back face of the prism, it excites a surface plasmon polariton at a critical angle so that the light that exits the prism serves as an intensity-modulated signal. The angle at which light couples to the plasmon polariton is determined by the reflection of an electromagnetic field at a metal–dielectric interface (with the prism as layer 1, the metal film as layer 2, and the sample to be sensed as layer 3) given by¹⁴

$$r = \frac{r_{12} + r_{23}e^{2ik_{z2}d}}{1 + r_{12}r_{23}e^{2ik_{z2}d}} \quad (1)$$

with metal thickness d and reflection coefficient between the i th and j th layer r_{ij} given by

$$r_{ij} = \frac{Z_i - Z_j}{Z_i + Z_j} \quad (2)$$

Here, $Z_i = \varepsilon_i/k_{zi}$ for p-polarized light and $k_{zi} = k_0(\varepsilon_i - \varepsilon_1) \sin^2(\theta_{\text{inc}})^{1/2}$ is the normal component of the wave vector in the metal layer that essentially contains angle of incidence information. s-Polarized light cannot excite a surface plasmon polariton in this geometry, but p-polarized light will be absorbed by surface plasmon polaritons at a critical angle that is strongly dependent on ε_3 . Because the index of refraction is proportional to the concentration of particles of interest in many solutions,^{24,25} the inferred shift in index can be used to determine a change in concentration of the analyte of interest.

The precision with which an angular shift can be determined is limited by the total noise of the sensing platform, but state-of-the-art SPR sensors are now at their classical limits where the SNL dominates the noise,¹² provided that the readout field does not feed noise into the index of refraction itself via nonlinear interactions or photothermal damage. This noise directly affects the sensitivity of the SPR sensor, since resonance shifts that are smaller than the noise cannot be resolved, meaning that the shot noise imposes a lower limit to the concentration of a specific analyte that a particular sensor can detect.

Figure 1b schematically illustrates this concept. In the upper plot, the line thickness represents the uncertainty in a measurement of the optical intensity for a shot noise limited SPR sensor. For very small shifts in the resonance, the lines are difficult to distinguish from one another. Either a higher confidence level (larger index shift) or longer integration time is necessary to discern them. When the noise floor is reduced via squeezing, changes in the reflected signal are easier to discern for the same confidence level or integration time.

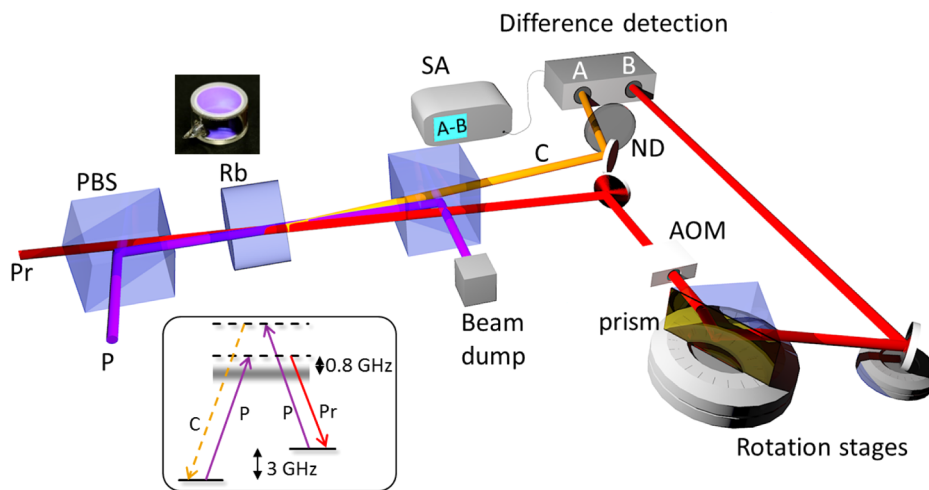


Figure 2. Experimental configuration for sub-SNL plasmonic sensing. A nonlinear optical process (four-wave mixing) in Rb vapor governed by a double- Λ scheme (inset) in the presence of a strong pump (P, purple) is used to produce probe (Pr, red) and conjugate (C, orange) beams for the SPR sensor. The conjugate field is used as the reference for subtracting classical and quantum noise, while the probe is used for optical readout. The detector takes the difference between the probe and conjugate intensities and displays the result on a spectrum analyzer. PBS: polarizing beam splitter; SA: spectrum analyzer; ND: variable neutral density filter; AOM: acousto-optic modulator.

Quantum noise reduction provides a higher SNR than is possible with a classical sensor, enabling the detection of smaller resonance shifts and thereby the inference of smaller concentrations of trace biochemical compounds.

Figure 2 shows a differential detection setup in which a reference beam (orange) is used to cancel the noise in the readout beam (red). The readout beam interacts with the plasmonic medium, while the reference beam is attenuated in order to cancel out the excess noise associated with both beams (the attenuation can be implemented optically or electronically). For beams sharing classical correlations, the measurement technique is shot noise limited provided that the common mode noise in each beam does not exceed the rejection ratio of the detector.^{13,14,16} However, by replacing the classical reference field with a mode that is quantum correlated with the readout field as shown in Figure 2, signals with noise levels below the SNL can be observed.

A highly accessible technique to generate these quantum-correlated fields is shown in Figure 2. A pump–probe experiment is conducted in a ⁸⁵Rb vapor cell at the D1 line, ~795 nm (inset of Figure 2^{19,20}). The pump field (P) excites atoms from both hyperfine ground states. Despite being off-resonance, a large pump power of approximately 300 mW ensures that the pump’s Rabi frequency is large enough to induce coherence between the hyperfine sublevels. A probe photon (Pr) closer to resonance stimulates emission of a photon from the coherently excited population preferentially into one of the ground-state sublevels, which requires that a second photon (called the conjugate, C) also be emitted in order to satisfy momentum and energy conservation while the coherence is preserved. The entire process, called four-wave mixing, is governed by a third-order nonlinear susceptibility, but the large intensity of the pump field combined with its undepleted amplitude ensures that the system behaves with characteristics similar to second-order parametric amplifiers. Since the number of probe photons emitted requires an equal number of conjugate photons to be emitted, the two fields share quantum intensity correlations, and a measurement of the intensity difference reveals reduced intensity-difference noise fluctuations compared to the SNL.^{19,20} This “two-mode squeezed state” or “twin beam” state has reduced noise in exactly the variable of detection associated with the shot noise limited Kretschmann geometry, that is, the intensity difference between the reference and readout beams. The noise floor is derived in the Supporting Information and is given in shot noise units by

$$\Delta N_-^2 = 1 - \frac{2\eta(G-1)}{2G-1} \quad (3)$$

where N_- is the photon number difference, η is the total transmission of both beams to a photodetector, including the detector’s quantum efficiency, and G is the nonlinear gain in the four-wave mixing interaction. Notably, the noise is less than one shot noise unit for $\eta > 0$ and $G > 1$. Thus, using this twin beam configuration in lieu of a traditional reference subtraction on a balanced detector will yield a signal-to-noise ratio increased by $2\eta(G-1)/(2G-1)$ over the shot-noise-limited measurement.^{19,20}

We experimentally implemented such a Kretschmann sensor with differential detection and quantum correlated beams using the process outlined above in order to directly detect shifts in the local index of refraction of calibrated index matching oils tuned to emulate flow cell operation. The probe field from the

four-wave mixing process was used as the readout beam in the SPR sensor, while the conjugate field was sent on to the balanced detector in order to cancel the quantum noise present in the probe field.

An acousto-optic modulator was used to place a modulation on the probe field so that both the signal and the intensity difference noise floor could be observed directly on a spectrum analyzer simultaneously, as shown in Figure 4b and c. The

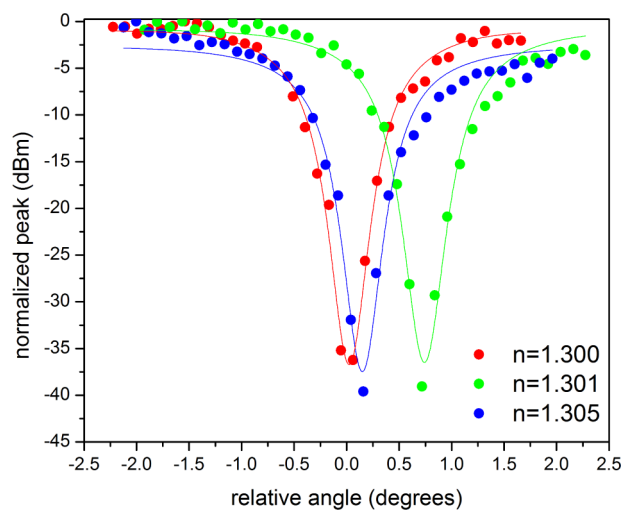


Figure 3. (a) Plasmonic resonance as a function of relative angle of incidence (0° corresponds to on-resonance for $n = 1.3$) and index of refraction (green: $n = 1.305$; blue: $n = 1.301$; red: $n = 1.300$). The numerical curve fits are intended as a guide to the eye.

amplitude of the modulation provided a direct measure of the reflected signal amplitude, and the noise floor surrounding the modulation is equivalent to the variance of a signal recorded at dc in conventional SPR spectroscopy, albeit with quantum noise reduction reducing the noise floor below the SNL. Applying a modulation and then demodulating (via either a spectrum analyzer or lock-in amplifier) has the added benefit of removing technical noise at dc that often exceeds the common mode rejection of balanced detectors under typical experimental conditions. The probe angle of incidence at the gold film was scanned by rotating a servo-controlled stage below the prism, while a mirror was counter-rotated at the opposite angle in order to ensure maximum transmission to the detector. The variable neutral density (ND) filter in the conjugate beam was rotated for each data point in order to ensure maximum noise cancellation.

At a specific angle for a given index of refraction, n , the reflectivity reaches a minimum. A shift in the position of this minimum can be used to infer the index of refraction, but the inflection point provides the greatest sensitivity to changes in index.¹³ Figure 3 shows the reflectivity as a function of angle for $n = 1.300$, 1.301 , and 1.305 , where the angle relative to the plasmon resonance for $n = 1.3$ is measured. Each data point in Figure 3 corresponds to the height of the modulation peak as viewed on the spectrum analyzer. Under attenuation a classical signal decreases more quickly than quantum noise, and the SNR of each peak in Figure 3 decreases closer to resonance. The amount of quantum noise reduction for each point along the angle scan is shown in Figure 4. It is clear from the figure that every point on each index scan shows quantum noise reduction. Figure 4b and c show the raw data on a spectrum

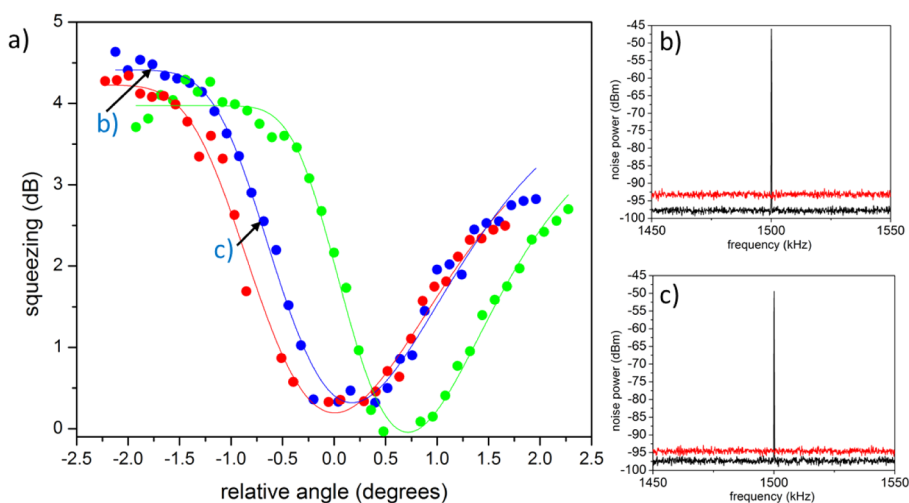


Figure 4. (a) Quantum noise reduction as a function of angle of incidence and index of refraction (green: $n = 1.305$; blue: $n = 1.301$; red: $n = 1.300$). (b and c) Raw data for two points along the curve. The red line indicates the shot noise level, while the peak is associated with the transmitted probe power. The sidebands that indicate the noise floor associated with each data point fall below the SNL; squeezing is equal to the difference between the black and red sidebands. Squeezing decreases as transmission decreases, but virtually all data points are squeezed. A maximum of 4.6 dB below the SNL is observed in the peak shoulders. A minimum of 0.3 dB is observed in the $n = 1.300$ and $n = 1.301$ data sets, while the $n = 1.305$ data set minimum is at the SNL.

analyzer associated with two data points in the scan (indicating approximately 4.5 dB of squeezing on the shoulder and 2.5 dB of squeezing at the inflection point). The peak heights in Figure 4b and c correspond to the magnitude of amplitude modulation on the probe field, and its maximum is located at the modulation frequency (1.5 MHz). Thus, reading the peak height is an effective signal demodulation, which is proportional to the intensity reaching the detector, while the sidebands correspond exactly to the noise floor associated with each measurement. The variance is proportional to the average of these noise sidebands; a lower noise sideband for a given peak height indicates a larger signal-to-noise ratio. The red lines in the insets of Figure 4 correspond to the measured SNL at each data point for the same optical power. A modulation peak with noise sidebands given by the red shot noise trace has a lower SNR than the peak associated with the squeezed (black) noise sidebands, and this is the case for every data point in the curves.

A large amount of squeezing is observed near the inflection points, meaning that one can choose to operate this SPR sensor at a single angle,¹³ where a large quantum effect is observed, and monitor the transmission as a function of time as the analyte concentration is varied, and at all points a higher SNR would be achieved than is possible with the classical version of this sensor. The index shift measured here (0.001) is the smallest observed to date using quantum states of light to interact with SPR sensors, but more importantly, the quantum fields themselves are bright beams, consisting of on the order of ~ 1 mW in general before absorption by the plasmonic sensor. The index shift here resulted in a very large angular shift in the plasmonic resonance, meaning that the sensor is likely capable of measuring several orders of magnitude smaller shifts, but the resolution of available calibrated oils prevented us from studying smaller shifts. Nonetheless, Figures 3 and 4 make it clear that when operating an optimal, shot-noise-limited classical sensor, twin beams automatically improve the SNR by the amount of quantum noise reduction present. In the optimum classical SPR sensor based on transmitted intensity, the lowest detectable shift reaches 10^{-7} refractive index units (RIU).¹² Our experimental results provide ~ 2.5 dB improve-

ment in the noise floor for such a measurement. This corresponds to a potential improvement in the smallest resolvable shift by 50%. For optimum, state of the art squeezed light sources with >10 dB of quantum noise reduction²⁶ and for minimal losses inside the sensor on par with the $\sim 92\%$ demonstrated here, SNRs could be increased dramatically, leading to a potential reduction in the lower limit of detection by an order of magnitude.

It is interesting to compare a sensor that uses quantum noise reduction to one that operates at the SNL, but with increased optical power to obtain the same improvement in SNR. First, we note that the quantum light source used here can operate at powers ranging from vacuum to >10 mW total while maintaining quantum noise reduction.¹⁰ Theoretically, the amount of quantum noise reduction does not depend on the incident optical power. Thus, one can envision operating a quantum noise reduction source with the same optical power that a classical sensor is capable of providing. It is clear that quantum noise reduction becomes important in power-constrained environments, such as when the medium under study is sensitive to high intensities and may become damaged. At the same low power levels, the SNL is larger in proportion to the signal, resulting in lower SNR than in higher power configurations. On the other hand, one may not increase optical power beyond the point of thermal modulation²⁷ of the plasmon or the damage threshold of photosensitive ligands,^{28,29} at which point the SPR device will cease to function as a linear index of refraction sensor. At powers just below those thresholds, the noise floor can be improved upon only by utilizing squeezed light. The SNR may also be improved by increasing the response of the plasmon to a local index change, for example, by introducing nanostructured surfaces or novel plasmonic materials.³⁰ For any possible configuration, the application of squeezed light as demonstrated here can be used to reduce the noise floor and further improve the SNR, demonstrating that the optimal measurement therefore always uses quantum noise reduction.

We also note that interferometric measurements are more sensitive than intensity-based measurements, and an intensity-

squeezed SPR sensor may not necessarily beat the SNR of a Mach–Zehnder-based phase-sensitive SPR sensor. However, it is clear that squeezed interferometers can also be used as quantum sensors,^{3,4} where all of the same arguments as above apply. In fact, utilizing more sensitive nonlinear interferometers^{31,32} leads to an even higher SNR than classical interferometric measurements. The use of such a device to register shifts in the plasmonic resonance as a function of index of refraction is currently under study and will be presented elsewhere.

In conclusion, we have demonstrated a squeezed SPR sensor in the Kretschmann configuration that was used to measure actual shifts in the plasmonic resonance as a function of a real index of refraction change. This constitutes the first quantum plasmonic sensor operating with bright optical powers with sensitivities that are scalable beyond the most sensitive classical measurements. These SPR sensors have been shown to be useful platforms for label-free detection, and the same techniques demonstrated here could be applied to arbitrarily functionalized SPR sensors.

■ ASSOCIATED CONTENT

📄 Supporting Information

The Supporting Information is available free of charge on the ACS Publications website at DOI: 10.1021/acsphtonic.5b00501.

Derivation of eq 3 describing squeezing in the presence of loss for a nonlinear amplifier (PDF)

■ AUTHOR INFORMATION

Corresponding Author

*E-mail: pooserrc@ornl.gov.

Notes

The authors declare no competing financial interest.

■ ACKNOWLEDGMENTS

This Letter has been authored by UT-Battelle, LLC under Contract No. DE-AC05-00OR22725 with the U.S. Department of Energy. The United States Government retains and the publisher, by accepting the article for publication, acknowledges that the United States Government retains a nonexclusive, paid-up, irrevocable, worldwide license to publish or reproduce the published form of this manuscript, or allow others to do so, for United States Government purposes. The Department of Energy will provide public access to these results of federally sponsored research in accordance with the DOE Public Access Plan (<http://energy.gov/downloads/doe-public-access-plan>). The authors acknowledge Jason Schaake and Roderick Davidson for thin film deposition. The metal film vapor deposition was carried out in the clean room facility at the Center for Nanophase Material Science (CNMS), a Department of Energy Office of Science user facility. The authors acknowledge support from the ORNL Laboratory directed research and development program (LDRD).

■ REFERENCES

- (1) Ye, J.; Kimble, H.; Katori, H. Quantum state engineering and precision metrology using state-insensitive light traps. *Science* **2008**, *320*, 1734–1738.
- (2) Meiser, D.; Ye, J.; Holland, M. Spin squeezing in optical lattice clocks via lattice-based QND measurements. *New J. Phys.* **2008**, *10*, 073014.

(3) Caves, C. M. Quantum-mechanical noise in an interferometer. *Phys. Rev. D: Part. Fields* **1981**, *23*, 1693–1708.

(4) Schnabel, R.; Mavalvala, N.; McClelland, D. E.; Lam, P. K. Quantum metrology for gravitational wave astronomy. *Nat. Commun.* **2010**, *1*, 121.

(5) Grote, H.; Danzmann, K.; Dooley, K. L.; Schnabel, R.; Slutsky, J.; Vahlbruch, H. First Long-Term Application of Squeezed States of Light in a Gravitational-Wave Observatory. *Phys. Rev. Lett.* **2013**, *110*, 181101.

(6) Taylor, M. A.; Janousek, J.; Daria, V.; Knittel, J.; Hage, B.; Bachor, H.-A.; Bowen, W. P. Biological measurement beyond the quantum limit. *Nat. Photonics* **2013**, *7*, 229–233.

(7) Lawrie, B. J.; Evans, P. G.; Pooser, R. C. Extraordinary Optical Transmission of Multimode Quantum Correlations via Localized Surface Plasmons. *Phys. Rev. Lett.* **2013**, *110*, 156802.

(8) Hoff, U. B.; Harris, G. I.; Madsen, L. S.; Kerdoncuff, H.; Lassen, M.; Nielsen, B. M.; Bowen, W. P.; Andersen, U. L. Quantum-enhanced micromechanical displacement sensitivity. *Opt. Lett.* **2013**, *38*, 1413–1415.

(9) Pooser, R. C.; Lawrie, B. Ultrasensitive measurement of microcantilever displacement below the shot-noise limit. *Optica* **2015**, *2*, 393–399.

(10) Lawrie, B. J.; Pooser, R. C. Toward real-time quantum imaging with a single pixel camera. *Opt. Express* **2013**, *21*, 7549–7559.

(11) Otterstrom, N.; Pooser, R. C.; Lawrie, B. J. Nonlinear optical magnetometry with accessible in situ optical squeezing. *Opt. Lett.* **2014**, *39*, 6533–6536.

(12) Piliarik, M.; Homola, J. Surface plasmon resonance (SPR) sensors: approaching their limits? *Opt. Express* **2009**, *17*, 16505–16517.

(13) Wang, X.; Jefferson, M.; Hobbs, P. C.; Risk, W. P.; Feller, B. E.; Miller, R. D.; Knoesen, A. Shot-noise limited detection for surface plasmon sensing. *Opt. Express* **2011**, *19*, 107–117.

(14) Wu, S. Y.; Ho, H. P.; Law, W. C.; Lin, C.; Kong, S. K. Highly sensitive differential phase-sensitive surface plasmon resonance biosensor based on the Mach-Zehnder configuration. *Opt. Lett.* **2004**, *29*, 2378–2380.

(15) Kalashnikov, D. A.; Pan, Z.; Kuznetsov, A. I.; Krivitsky, L. A. Quantum spectroscopy of plasmonic nanostructures. *Phys. Rev. X* **2014**, *4*, 011049.

(16) Blanchard-Dionne, A.; Guyot, L.; Patskovsky, S.; Gordon, R.; Meunier, M. Intensity based surface plasmon resonance sensor using a nanohole rectangular array. *Opt. Express* **2011**, *19*, 15041–15046.

(17) Takada, K.; Himeno, A.; Yukimatsu, K. Phase-noise and shot-noise limited operations of low coherence optical time domain reflectometry. *Appl. Phys. Lett.* **1991**, *59*, 2483–2485.

(18) Durry, G.; Pouchet, I.; Amarouche, N.; Danguy, T.; Megie, G. Shot-noise-limited dual-beam detector for atmospheric trace-gas monitoring with near-infrared diode lasers. *Appl. Opt.* **2000**, *39*, 5609–5619.

(19) McCormick, C. F.; Boyer, V.; Arimondo, E.; Lett, P. D. Strong relative intensity squeezing by four-wave mixing in rubidium vapor. *Opt. Lett.* **2007**, *32*, 178–180.

(20) Boyer, V.; Marino, A. M.; Pooser, R. C.; Lett, P. D. Entangled Images from Four-Wave Mixing. *Science* **2008**, *321*, 544–547.

(21) Tame, M.; McEneaney, K.; Özdemir, Ş.; Lee, J.; Maier, S.; Kim, M. Quantum plasmonics. *Nat. Phys.* **2013**, *9*, 329–340.

(22) Huck, A.; Smolka, S.; Lodahl, P.; Sørensen, A. S.; Boltasseva, A.; Janousek, J.; Andersen, U. L. Demonstration of quadrature-squeezed surface plasmons in a gold waveguide. *Phys. Rev. Lett.* **2009**, *102*, 246802.

(23) Kretschmann, E. The determination of the optical constants of metals by excitation of surface plasmons. *Eur. Phys. J. A* **1971**, *241*, 313–324.

(24) Strop, P.; Brunger, A. T. Refractive index-based determination of detergent concentration and its application to the study of membrane proteins. *Protein Sci.* **2005**, *14*, 2207–2211.

(25) Stenberg, E.; Persson, B.; Roos, H.; Urbaniczky, C. Quantitative determination of surface concentration of protein with surface

plasmon resonance using radiolabeled proteins. *J. Colloid Interface Sci.* **1991**, *143*, 513–526.

(26) Eberle, T.; Steinlechner, S.; Bauchrowitz, J.; Händchen, V.; Vahlbruch, H.; Mehmet, M.; Müller-Ebhardt, H.; Schnabel, R. Quantum Enhancement of the Zero-Area Sagnac Interferometer Topology for Gravitational Wave Detection. *Phys. Rev. Lett.* **2010**, *104*, 251102.

(27) Kaya, S.; Weeber, J.-C.; Zacharatos, F.; Hassan, K.; Bernardin, T.; Cluzel, B.; Fatome, J.; Finot, C. Photo-thermal modulation of surface plasmon polariton propagation at telecommunication wavelengths. *Opt. Express* **2013**, *21*, 22269–22284.

(28) Robinson, H. D.; Magill, B. A.; Guo, X.; Reyes, R. L.; See, E. M.; Davis, R. M.; Santos, W. L. Two-photon activation of o-nitrobenzyl ligands bound to gold surfaces. *Proc. SPIE* **2014**, 916336–916336.

(29) Bartczak, D.; Muskens, O. L.; Millar, T. M.; Sanchez-Elsner, T.; Kanaras, A. G. Laser-induced damage and recovery of plasmonically targeted human endothelial cells. *Nano Lett.* **2011**, *11*, 1358–1363.

(30) West, P. R.; Ishii, S.; Naik, G. V.; Emani, N. K.; Shalaev, V. M.; Boltasseva, A. Searching for better plasmonic materials. *Laser & Photonics Reviews* **2010**, *4*, 795–808.

(31) Hudelist, F.; Kong, J.; Liu, C.; Jing, J.; Ou, Z.; Zhang, W. Quantum metrology with parametric amplifier-based photon correlation interferometers. *Nat. Commun.* **2014**, *5*.

(32) Marino, A. M.; Corzo Trejo, N. V.; Lett, P. D. Effect of losses on the performance of an SU(1,1) interferometer. *Phys. Rev. A: At., Mol., Opt. Phys.* **2012**, *86*, 023844.